Coadsorption of two monomer species on a square lattice with first- and second-neighbor interactions

Alain J. Phares, Francis J. Wunderlich, Joseph P. Martin, Patrick M. Burns, and Gintaras K. Duda
Department of Physics, Mendel Hall, Villanova University, Villanova, Pennsylvania 19085-1699
(Received 18 April 1997)

We obtain the low-temperature phases and phase transitions of the coadsorption of two monomer species on a semi-infinite square lattice of odd width M, with first- and second-neighbor interactions. We study the cases for which first-neighbor interactions between two monomers of the same species are repulsive, allowing all other interactions to be attractive or repulsive. Most of the numerical results are found to fit exact closed-form expressions in M, thus allowing exact analytic extrapolations to the infinite two-dimensional case ($M=\infty$). [S1063-651X(97)05508-6]

PACS number(s): 02.50.−r, 05.50.+q, 05.70.−a, 64.60.Cn

I. INTRODUCTION

While no exact solution of lattice models for the adsorption or coadsorption of gas molecules on surfaces has been analytically derived, when first- and second-neighbor interactions between the adsorbed molecules are considered, low-temperature numerical studies of one species of monomers adsorbed on a square lattice allow one to obtain closed-form analytic expressions for all possible phases and for the conditions under which phase transitions occur [1]. In this previous work, the surface considered was a semi-infinite $M\times N$ square lattice ($N\rightarrow\infty$) in the presence of a gas containing one molecular species, with the adsorbed molecules each occupying one site. For this reason, we referred to them as monomers. The system is at thermal equilibrium with the monomer chemical potential energy μ depending on the external gas pressure. The interaction energies of an adsorbed monomer are V_0 with the lattice, V with any first-neighbor monomer at a distance a, and W with any second-neighbor monomer at a distance $a\sqrt{2}$. The assumption was that the first-neighbor interaction is repulsive, $V<0$, allowing the second-neighbor interaction to be either attractive or repulsive. The study showed six distinct interaction regions with ''p phases'' appearing sequentially with increasing external pressure, from the empty lattice phase p_0 to the fully covered lattice phase p_{15}, as follows [1].

Region (a). For M odd, $V<W\leqslant V/2$ with phases p_1,p_8,p_{13},p_{15}, and for M even, $V<W<V/2$ with phases $p_1,p_4,p_8,p_9,p_{13},p_{14},p_{15}$.

Region (b). For M odd, $V/2<W<(V/2)(M-2)/(M-1)$ with phases $p_1,p_5,p_6,p_8,p_{13},p_{15}$.

Region (b′). For M even, $W=V/2$ with phases $p_1,p_3,p_7,p_{10},p_{12},p_{14},p_{15}$.

Region (c). $(V/2)(M-2)/(M-1)\leqslant W<0$ for M odd with phases $p_1,p_5,p_6,p_{13},p_{15}$ and for M even with phases $p_1,p_2,p_5,p_8,p_{11},p_{14},p_{15}$.

Region (d). $0\leqslant W<-(V/2)(M-2)/(M-1)$ with phases p_5,p_6,p_{15}.

Region (e). $-(V/2)(M-2)/(M-1)\leqslant W$ with phases p_5,p_{15}.

The exact analytical results obtained for any finite width M of the lattice are particularly relevant to adsorption on terraces, and special attention was given to edge effects. Exact analytic extrapolation to the infinite two-dimensional lattice ($M\rightarrow\infty$) was straightforward, and the results for even and odd values of M were verified to converge to the same limit.

In the present study of coadsorption of two distinct molecular species, we consider lattices of odd width M only, and results for the infinite two-dimensional lattice are obtained by allowing M odd to become infinite. Since one expects the existence of phases where the lattice is covered by only one species, the corresponding phases are called p and q phases for the first and second species, respectively. The ordering index for the q phases is the same as that of the p phases. Table I provides the characteristics of the p and q phases appearing for M odd, as found in Ref. [1]. Phases p_0 and q_0 refer to the same ''empty lattice'' phase, which we now call the E phase, and the following paragraphs provide the significance of the vertical entries found in Table I.

In our model, the coadsorption of two molecular species with first- and second-neighbor interactions involves eight interaction energies: V_{10} and V_{20} are the interaction energies with the lattice of monomers of the first species (index 1) and second species (index 2), respectively; V_{11}, V_{22}, and V_{12} are the first-neighbor interaction energies between the adsorbed molecular species, first-first species, second-second species, and first-second species, respectively; and W_{11}, W_{22}, and W_{12} are the second-neighbor interaction energies between the adsorbed molecular species, first-first species, second-second species, and first-second species, respectively. The chemical potential energies μ_1 and μ_2 of the corresponding monomer species may be varied by changing the respective species' partial pressure in the gas phase. The relevant eight activities associated with this system are

$$x_i=\exp\left[\frac{\mu_i+V_{i0}}{k_BT}\right],$$
$$y_{ij}=\exp\left[\frac{V_{ij}}{k_BT}\right], \tag{1}$$
$$z_{ij}=\exp\left[\frac{W_{ij}}{k_BT}\right],$$

TABLE I. Occupational characteristics of the phases of one monomer species on a square lattice of odd width M. The p and q phases refer to monomers of the first and second species.

Phase	θ_{10}	θ_{20}	θ_{11}	θ_{22}	θ_{12}	β_{11}	β_{22}	β_{12}
E	0	0	0	0	0	0	0	0
p_1	$\frac{M+1}{4M}$	0	0	0	0	0	0	0
p_5	$\frac{1}{2}$	0	0	0	0	$\frac{M-1}{M}$	0	0
p_6	$\frac{M+1}{2M}$	0	$\frac{M+1}{2M}$	0	0	0	0	0
p_8	$\frac{M+2}{2M}$	0	$\frac{3}{M}$	0	0	$\frac{M-1}{M}$	0	0
p_{13}	$\frac{3M+1}{4M}$	0	1	0	0	$\frac{M-1}{M}$	0	0
p_{15}	1	0	$\frac{2M-1}{M}$	0	0	$\frac{2M-2}{M}$	0	0
q_1	0	$\frac{M+1}{4M}$	0	0	0	0	0	0
q_5	0	$\frac{1}{2}$	0	0	0	0	$\frac{M-1}{M}$	0
q_6	0	$\frac{M+1}{2M}$	0	$\frac{M+1}{2M}$	0	0	0	0
q_8	0	$\frac{M+2}{2M}$	0	$\frac{3}{M}$	0	0	$\frac{M-1}{M}$	0
q_{13}	0	$\frac{3M+1}{4M}$	0	1	0	0	$\frac{M-1}{M}$	0
q_{15}	0	1	0	$\frac{2M-1}{M}$	0	0	$\frac{2M-2}{M}$	0

where k_B is Boltzmann's constant and T the absolute temperature. Here the transfer matrix T_M^1 for a lattice of width M is of rank $D(M)=3^M$. It is recursively constructed as in Refs. [1,2], and we find

$$T_M^1=\begin{pmatrix} T_{M-1}^1 & x_1P_{M-1}^1 & x_2Q_{M-1}^1 \\ T_{M-1}^2 & x_1y_{11}P_{M-1}^2 & x_2y_{12}Q_{M-1}^2 \\ T_{M-1}^3 & x_1y_{12}P_{M-1}^3 & x_2y_{22}Q_{M-1}^3 \end{pmatrix}, \tag{2a}$$

$$T_M^2=\begin{pmatrix} T_{M-1}^1 & x_1z_{11}P_{M-1}^1 & x_2z_{12}Q_{M-1}^1 \\ T_{M-1}^2 & x_1y_{11}z_{11}P_{M-1}^2 & x_2y_{12}z_{12}Q_{M-1}^2 \\ T_{M-1}^3 & x_1y_{12}z_{11}P_{M-1}^2 & x_2y_{22}z_{12}Q_{M-1}^3 \end{pmatrix}, \tag{2b}$$

$$T_M^3=\begin{pmatrix} T_{M-1}^1 & x_1z_{12}P_{M-1}^1 & x_2z_{22}Q_{M-1}^1 \\ T_{M-1}^2 & x_1y_{11}z_{12}P_{M-1}^2 & x_2y_{12}z_{22}Q_{M-1}^2 \\ T_{M-1}^3 & x_1y_{12}z_{12}P_{M-1}^2 & x_2y_{22}z_{22}Q_{M-1}^3 \end{pmatrix}. \tag{2c}$$

Each of the matrices P_M^i $(i=1,2,3)$ is obtained from the above block form expression of the corresponding T_M^i by multiplying all its block matrices in the second and third columns by y_{11} and y_{12}, respectively, and also by multiplying all its block matrices in the second and third rows by z_{11} and z_{12}, respectively. Each of the matrices Q_M^i is obtained from the expression of the corresponding T_M^i by multiplying all its block matrices in the second and third columns by y_{12} and y_{22}, respectively, and also by multiplying all its block matrices in the second and third rows by z_{12} and z_{22}, respectively. The initial conditions are

$$T_0^i=P_0^i=Q_0^i=1. \tag{3}$$

The fraction of the lattice that is occupied by the monomers of the first species is θ_{10} and that of the second species is θ_{20}. The number per site of first-neighbor adsorbate (i) to adsorbate (j) is denoted θ_{ij}. Similarly, the number per site of second-neighbor adsorbate (i) to adsorbate (j) is β_{ij}. In the limit $N\to\infty$, these quantities are related to the largest eigenvalue R of T_M^1 according to

$$\theta_{i0}=\frac{x_i}{MR}\frac{\partial R}{\partial x_i},\quad \theta_{ij}=\frac{y_{ij}}{MR}\frac{\partial R}{\partial y_{ij}},\quad \beta_{ij}=\frac{z_{ij}}{MR}\frac{\partial R}{\partial z_{ij}},$$
$$S=\frac{1}{M}\ln R-\sum_i \theta_{i0}\ln x_i-\sum_{i\leqslant j}\theta_{ij}\ln y_{ij}-\sum_{i\leqslant j}\beta_{ij}\ln z_{ij}, \tag{4}$$

where S is the entropy per site divided by k_B. For finite length N of the lattice, all the eigenvalues contribute to the expressions of θ_{i0}, θ_{ij}, β_{ij}, and S in a manner that is similar to the one discussed in Ref. [3]. Consider a given coad-

sorption system corresponding to given interaction energies V_{ij} and W_{ij} and with the temperature of the system set to be below a certain value as dictated by the relation

$$\frac{I}{k_B T} < 10 \Rightarrow T < \frac{I}{10 k_B}, \tag{5}$$

where I stands for the absolute value of the lowest of the first-neighbor interaction energies. Adsorption patterns are numerically studied by increasing either of the two external chemical potential energies, keeping the other fixed. The Cray C90 of the Pittsburgh Supercomputing Center is used with EISPACK for the numerical computations.

The energy per site must be continuous across a phase boundary. Thus, with $\Delta\theta_{10}$, $\Delta\theta_{20}$, $\Delta\theta_{11}$, $\Delta\theta_{22}$, $\Delta\theta_{12}$, $\Delta\beta_{11}$, $\Delta\beta_{22}$, and $\Delta\beta_{12}$ being the corresponding changes across a given boundary of θ_{10}, θ_{20}, θ_{11}, θ_{22}, θ_{12}, β_{11}, β_{22}, and β_{12}, no change in the energy per site requires

$$\sum_i (\mu_i + V_{i0}) \Delta\theta_{i0} + \sum_{i \leqslant j} (V_{ij} \Delta\theta_{ij} + W_{ij} \Delta\beta_{ij}) = 0. \tag{6}$$

This equation has been numerically verified to hold in all cases.

Coadsorption on the one-dimensional lattice ($M=1$) is the only system for which an exact analytic solution can be derived. On this lattice, however, second neighbors are at distances $2a$ rather than $a\sqrt{2}$ and their interactions are neglected. The exact analytic solution follows from computing the eigenvalues of T_1^1 with $M=1$. These eigenvalues are the solutions of the cubic equation

$$\begin{aligned} R^3 - R^2(1 + x_1 y_{11} + x_2 y_{22}) + R[x_1 x_2 (y_{11} y_{22} - y_{12}) + x_1 y_{11} \\ + x_2 y_{22} - x_1 - x_2] + x_1 x_2 (y_{12}^2 - y_{11} y_{22} + y_{11} + y_{22} \\ - 2 y_{12}) = 0. \end{aligned} \tag{7}$$

Section II provides the lattice configurations and the characteristics of all the phases encountered for $M \geqslant 3$. Which phases and phase transitions are observed should depend on the first- and second-neighbor interaction energies. These questions are discussed in Sec. III, which also presents a selection of the cases investigated. Section IV gives a detailed analysis of two phase transitions for which exact analytic results were derived. Section V provides the limit as $M \to \infty$ and Sec. VI is the summary and conclusion.

II. LATTICE CONFIGURATIONS OF THE OBSERVED PHASES

The monomer species labeled 1 may have interaction energies that fall in one of the five energy regions listed above for M odd, namely, regions a, b, c, d, or e, generically called r; in a similar way, the monomer species labeled 2 have interaction energies that fall in one of these same regions. The notation used is as follows. Consider the case for which one has the monomer species of type 1 having interaction energies V_{11} and W_{11} falling in region r and those of type 2 having interaction energies V_{22} and W_{22} falling in region s. This case will be referred to as the one for which the coadsorption system belongs to the region r-s. The symmetry between regions r-s and s-r requires that there be fifteen distinct cases, five r-r and ten r-s cases with $r \neq s$. In each of these distinct cases, we have considered all possible orders of the set of values $V_{11}, W_{11}, V_{22}, W_{22}$. For example, one possible order is $V_{11} < V_{22} < W_{11} < W_{22}$. For a given order within a given r-s case, we have allowed first- and second-neighbor interaction energies V_{12} and W_{12} to be each either attractive or repulsive, with values within a reasonable range. Our numerical investigation covered the values of $M=3$, 5, and 7, for which the rank of the transfer matrix is 27, 243, and 2187, respectively. By $M=7$, the pattern had been established and there was no need to expend further computer time for $M>7$. As was the case with one species of monomer adsorption on lattices of odd width [1], all coadsorption phases were found to have a perfect structural ordering or zero entropy. We now present all the coadsorption phases we have encountered, including their characteristics and lattice configurations for any M odd.

When the molecules of one species are by far the most predominant in the gas phase, they are the only adsorbed species and the observed phases are either the p or the q phases listed in Table I. Table II provides the occupational characteristics of the observed P phases, which we have labeled a, for which the lattice of odd width M is *partially* covered by a mixture of monomers of the first and second species. The order of listing is by increasing first θ_{10}, then θ_{20}, and finally θ_{22}. In this table, exchanging indices 1 and 2 in the vertical entries generates the characteristics of ''dual'' P phases, labeled b, with $P10$ being its own dual, Thus the complete set of phases involving a mixture of monomers of both species partially covering the lattice includes 35 phases $P10$, $P1a$–$P9a$, $P11a$–$P18a$, $P1b$–$P9b$, and $P11b$–$P18b$. Using the same ordering, Table III provides the occupational characteristics of all the F phases labeled a and b for which the lattice of odd width M is *fully* covered by a mixture of both monomer species. There are 12 F phases: $F6$ and $F7$, which are their own dual, $F1a$–$F5a$, and their dual phases $F1b$–$F5b$. Since p and q phases have been discussed in Ref. [1], we present the lattice occupational configurations for P and F phases in Figs. 1 and 2, respectively. In these figures a square cell represents a lattice site. Either it is empty or it has a circle or a cross at its center, indicating a lattice site that is vacant or occupied by a monomer of the first or second species, respectively. Figure 1 provides the occupational configurations for the P phases labeled a. The configurations of their dual P phases are obtained by exchanging circles and crosses.

As mentioned earlier, we have investigated the 15 distinct energy regions r-s, each of which involves a number of possible cases. In the forthcoming section, we have selected three cases to exhibit the main features of this lattice model. In this selection we will show which phases are observed, and the conditions at the boundary between phases will be discussed.

III. PHASE DIAGRAMS

For convenience, we introduce energy parameters Y and X expressed in kelvin and given by

$$Y = (\mu_1 + V_{10})/k_B, \quad X = (\mu_2 + V_{20})/k_B. \tag{8}$$

TABLE II. Occupational characteristics of the coadsorption phases corresponding to partial covering of a square lattice of odd width M by two monomer species. This is a partial list of phases. The nonlisted phases are those for which the subscripts 1 and 2 of the vertical entries are interchanged.

Phase	θ_{10}	θ_{20}	θ_{11}	θ_{22}	θ_{12}	β_{11}	β_{22}	β_{12}
$P1a$	$\frac{1}{M}$	$\frac{M-2}{2M}$	0	0	0	0	$\frac{M-3}{M}$	$\frac{2}{M}$
$P2a$	$\frac{1}{M}$	$\frac{1}{2}$	0	0	$\frac{3}{M}$	0	$\frac{M-1}{M}$	0
$P3a$	$\frac{M-1}{4M}$	$\frac{M+1}{4M}$	0	0	0	0	0	$\frac{M-1}{M}$
$P4a$	$\frac{M-1}{4M}$	$\frac{M+5}{4M}$	0	$\frac{2}{M}$	$\frac{1}{M}$	0	0	$\frac{M-1}{M}$
$P5a$	$\frac{M-1}{4M}$	$\frac{1}{2}$	0	0	$\frac{M-1}{M}$	0	$\frac{M-1}{M}$	0
$P6a$	$\frac{M-1}{4M}$	$\frac{1}{2}$	0	$\frac{M-1}{2M}$	$\frac{M-1}{2M}$	0	0	$\frac{M-1}{M}$
$P7a$	$\frac{M-1}{4M}$	$\frac{M+1}{2M}$	0	$\frac{M+1}{2M}$	$\frac{M-1}{2M}$	0	0	$\frac{M-1}{M}$
$P8a$	$\frac{M-1}{4M}$	$\frac{M+2}{2M}$	0	$\frac{3}{M}$	$\frac{M-1}{M}$	0	$\frac{M-1}{M}$	$\frac{2}{M}$
$P9a$	$\frac{M-1}{4M}$	$\frac{3M-3}{4M}$	0	$\frac{M-3}{M}$	$\frac{M-1}{M}$	0	$\frac{M-1}{M}$	$\frac{M-3}{M}$
$P10$	$\frac{M+1}{4M}$	$\frac{M+1}{4M}$	0	0	$\frac{M+1}{2M}$	0	0	0
$P11a$	$\frac{M+1}{4M}$	$\frac{M+3}{4M}$	0	0	$\frac{3}{M}$	0	$\frac{2}{M}$	$\frac{M-3}{M}$
$P12a$	$\frac{M+1}{4M}$	$\frac{M+3}{4M}$	0	$\frac{1}{M}$	$\frac{2}{M}$	0	0	$\frac{M-1}{M}$
$P13a$	$\frac{M+1}{4M}$	$\frac{M-2}{2M}$	0	0	$\frac{M-3}{M}$	0	$\frac{M-3}{M}$	$\frac{2}{M}$
$P14a$	$\frac{M+1}{4M}$	$\frac{1}{2}$	0	0	1	0	$\frac{M-1}{M}$	0
$P15a$	$\frac{M+1}{4M}$	$\frac{1}{2}$	0	$\frac{M-1}{2M}$	$\frac{M+1}{2M}$	0	0	$\frac{M-1}{M}$
$P16a$	$\frac{M-2}{2M}$	$\frac{M+5}{4M}$	0	$\frac{2}{M}$	$\frac{M-2}{M}$	$\frac{M-3}{M}$	0	$\frac{2}{M}$
$P17a$	$\frac{M-2}{2M}$	$\frac{1}{2}$	0	0	$\frac{2M-4}{M}$	$\frac{M-3}{M}$	$\frac{M-1}{M}$	0
$P18a$	$\frac{M-2}{2M}$	$\frac{1}{2}$	0	$\frac{1}{M}$	$\frac{2M-5}{M}$	$\frac{M-3}{M}$	$\frac{M-3}{M}$	$\frac{2}{M}$

For a given set of two molecular species, the interaction energies are fixed and, at a sufficiently low temperature T, the quantities X and Y are varied by adjusting the respective partial pressure of the molecular species in the gas phase. In the plot of Y versus X, a number of low-temperature phases occur in certain regions. For the interaction energies mentioned above, the only phases observed are those presented in Sec. II. The interaction energies V_{ij} and W_{ij} dictate the phases that are observed in the XY plot, thereafter referred to as the phase diagram. In this diagram, the phase boundaries must be straight lines, as follows from combining Eqs. (6) and (8):

$$\begin{aligned} Y\Delta\theta_{10} = &-X\Delta\theta_{20}-(V_{11}/k_B)\Delta\theta_{11}-(V_{22}/k_B)\Delta\theta_{22} \\ &-(V_{12}/k_B)\Delta\theta_{22}-(W_{11}/k_B)\Delta\beta_{11}-(W_{22}/k_B)\Delta\beta_{22} \\ &-(W_{12}/k_B)\Delta\beta_{22}. \end{aligned} \tag{9}$$

TABLE III. Occupational characteristics of the coadsorption phases corresponding to full coverage of a square lattice of odd width M by two monomer species.

Phase	θ_{10}	θ_{20}	θ_{11}	θ_{22}	θ_{12}	β_{11}	β_{22}	β_{12}
$F1a$	$\frac{2}{M}$	$\frac{M-2}{M}$	$\frac{2}{M}$	$\frac{2M-5}{M}$	$\frac{2}{M}$	0	$\frac{2M-6}{M}$	$\frac{4}{M}$
$F2a$	$\frac{M-1}{4M}$	$\frac{3M+1}{4M}$	0	1	$\frac{M-1}{M}$	0	$\frac{M-1}{M}$	$\frac{M-1}{M}$
$F3a$	$\frac{M+1}{4M}$	$\frac{3M-1}{4M}$	0	$\frac{M-1}{M}$	1	0	$\frac{M-1}{M}$	$\frac{M-1}{M}$
$F4a$	$\frac{M-2}{2M}$	$\frac{M+2}{2M}$	0	$\frac{3}{M}$	$\frac{2M-4}{M}$	$\frac{M-3}{M}$	$\frac{M-1}{M}$	$\frac{2}{M}$
$F5a$	$\frac{M-1}{2M}$	$\frac{M+1}{2M}$	$\frac{M-1}{2M}$	$\frac{M+1}{2M}$	$\frac{M-1}{M}$	0	0	$\frac{2M-2}{M}$
$F6$	$\frac{1}{2}$	$\frac{1}{2}$	0	0	$\frac{2M-1}{M}$	$\frac{M-1}{M}$	$\frac{M-1}{M}$	0
$F7$	$\frac{1}{2}$	$\frac{1}{2}$	$\frac{M-1}{2M}$	$\frac{M-1}{2M}$	1	0	0	$\frac{2M-2}{M}$
$F5b$	$\frac{M+1}{2M}$	$\frac{M-1}{2M}$	$\frac{M+1}{2M}$	$\frac{M-1}{2M}$	$\frac{M-1}{M}$	0	0	$\frac{2M-2}{M}$
$F4b$	$\frac{M+2}{2M}$	$\frac{M-2}{2M}$	$\frac{3}{M}$	0	$\frac{2M-4}{M}$	$\frac{M-1}{M}$	$\frac{M-3}{M}$	$\frac{2}{M}$
$F3b$	$\frac{3M-1}{4M}$	$\frac{M+1}{4M}$	$\frac{M-1}{M}$	0	1	$\frac{M-1}{M}$	0	$\frac{M-1}{M}$
$F2b$	$\frac{3M+1}{4M}$	$\frac{M-1}{4M}$	1	0	$\frac{M-1}{M}$	$\frac{M-1}{M}$	0	$\frac{M-1}{M}$
$F1b$	$\frac{M-2}{M}$	$\frac{2}{M}$	$\frac{2M-5}{M}$	$\frac{2}{M}$	$\frac{2}{M}$	$\frac{2M-6}{M}$	0	$\frac{4}{M}$

In general, when the partial pressure of the second species is relatively low and, consequently, the value of X is mainly negative, the adsorbed molecules are those of the first species and the phases observed are those reported in Ref. [1] (p phases). In this case, $\theta_{20}=\theta_{22}=\theta_{12}=\beta_{22}=\beta_{12}=0$ and their corresponding changes are automatically zero. Thus, according to Eq. (9), phase boundaries in that region of the phase diagram are straight lines parallel to the X axis. Similarly, when the most abundant molecules in the gas phase are by far those of the second species, corresponding to the region where Y is mainly negative, the adsorption phases in this region are q phases and their mutual boundaries are straight lines parallel to the Y axis.

The phase diagrams of Figs. 3–5 are in units of 100 K. The numerical computations were conducted in the temperature range 30–100 K and the data were generated with a lattice width $M=5$. Figure 3 is a sample phase diagram for a coadsorption system belonging to region a-a with $V_{11}/k_B=-1800$ K, $V_{22}/k_B=-1400$ K, $V_{12}/k_B=-2000$ K, $W_{11}/k_B=-1600$ K, $W_{22}/k_B=-800$ K, and $W_{12}/k_B=-250$ K. Figure 4 is a sample from region a-c with $V_{11}/k_B=-1800$ K, $V_{22}/k_B=-1400$ K, $V_{12}/k_B=-300$ K, $W_{11}/k_B=-1600$ K, $W_{22}/k_B=-500$ K, and $W_{12}/k_B=-200$ K. Finally, Fig. 5 is a sample from region b-b with $V_{11}/k_B=-2400$ K, $V_{22}/k_B=-1600$ K, $V_{12}/k_B=1200$ K, $W_{11}/k_B=-1000$ K, $W_{22}/k_B=-700$ K, and $W_{12}/k_B=900$ K. One should note that temperature is a scaling factor. In the cases considered, energies are around 1000 K or of the order of 2 kcal/mole and the phases observed are at temperatures below 100 K. Should we have picked energies that are 10 times higher, the same phases would have been observed for temperatures below 1000 K. The regions encountered in these diagrams are named after their corresponding phases as found in Tables I–III. The boundary line equations are easily obtained by using these tables and Eq. (9). As expected, the p phases observed in the region of each phase diagram where X is mostly negative are dictated by the values assigned to V_{11} and W_{11} falling in the interaction energy region a or b. Similarly, the q phases observed in the region of each phase diagram where Y is mostly negative are dictated by the values assigned to V_{22} and W_{22} falling in the interaction energy regions a, c, and b, respectively. Figure 3, the sample from region a-a, exhibits phases appearing in dual pairs: the expected pairs (p_1,q_1), (p_8,q_8), (p_{13},q_{13}), and (p_{15},q_{15}) and five additional pairs $(P3a,P3b)$, $(P4a,P4b)$, $(P7a,P7b)$, and $(F5a,F5b)$. Figure 4, the sample from region a-c, also exhibits a certain symmetry. The p and q phases are those of regions a and c, respectively. With the exception of phase $F5b$, the remaining mixed P and F phases appear in dual pairs: $(P3a,P3b)$, $(P7a,P7b)$, $(P12a,P12b)$,

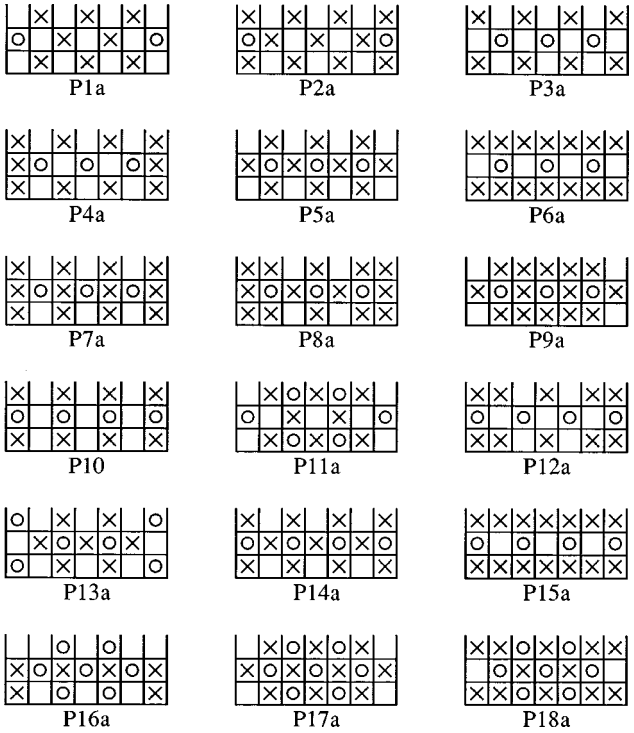

FIG. 1. Occupational configurations for the phases listed in Table II. A lattice site is represented by a square cell of size a, which is left blank when unoccupied and has a circle or a cross representing a monomer of the first or second species, respectively.

($P15a$,$P15b$), ($F2a$,$F2b$), and phase $F7$ is its own dual. Interestingly, Fig. 5, the sample from region b-b, is not completely symmetric in the appearance of its phases. The mixed phases appearing in dual pairs are ($P6a$,$P6b$), ($F2a$,$F2b$), ($F5a$,$F5b$), and $F7$, which is its own dual. The remaining mixed phases are $P3b$, $P7b$, and $P15a$.

In general, a boundary line between two phases has a slope of one when $\Delta\theta_{10}=-\Delta\theta_{20}$, as follows from Eq. (9). This is the case when the two phases correspond to a fully covered lattice ($\theta_{10}+\theta_{20}=1$) or when they are the dual of one another. For example, in Fig. 3, the boundary lines between $P3a$ and $P3b$, $P4a$ and $P4b$, $P7a$ and $P7b$, $F5a$ and $F5b$, $F5a$ and q_{15}, and $F5b$ and p_{15} all have a slope of one. A boundary line is vertical or horizontal, when the phases on either side have the same value of either θ_{10} or θ_{20}, respectively. These properties have been used as a check of the very high accuracy (better than ten figures) of our numerical computations. In all full coverage phases and at any boundary point on the boundary between any two such phases, simple counting of first and second neighbors per site on a lattice of width M requires

$$\theta_{11}+\theta_{22}+\theta_{12}=(2M-1)/M, \qquad (10)$$

$$\beta_{11}+\beta_{22}+\beta_{12}=(2M-2)/M.$$

This has also been used as still another check of the validity of our numerical results. Finally, we have also verified that one obtains the same set of values of S, θ_{ij}, and β_{ij} at any point on a boundary line between two phases.

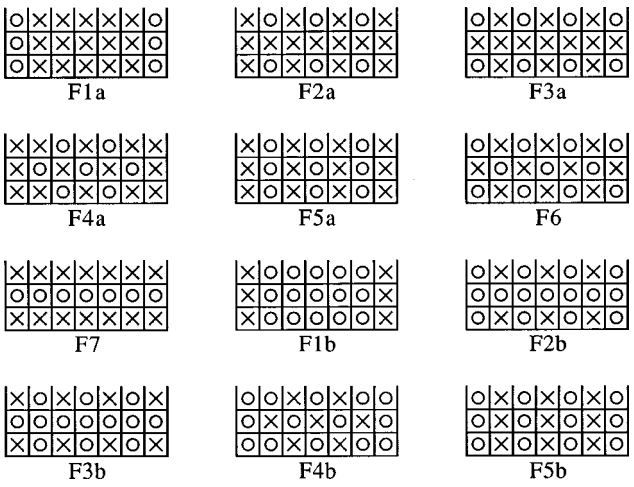

FIG. 2. Occupational configurations for the phases listed in Table III, with the same convention adopted in Fig. 1.

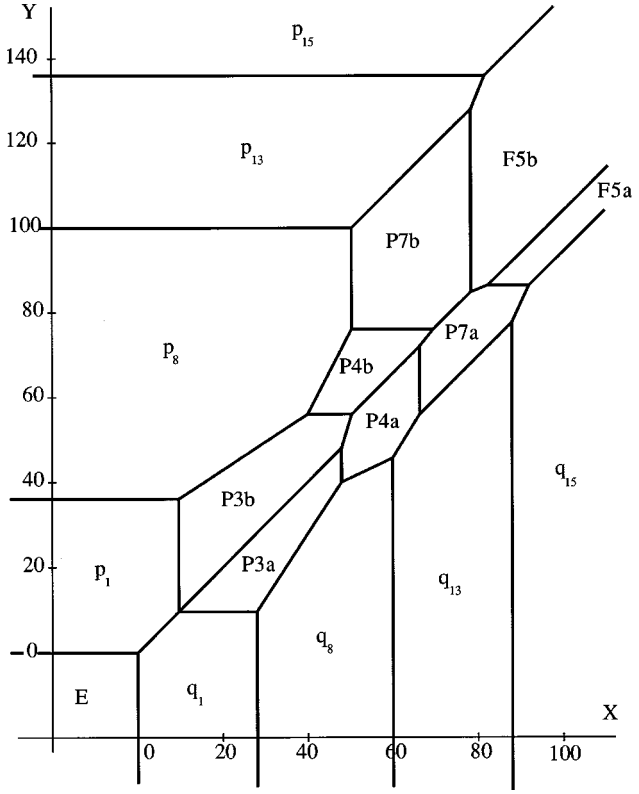

FIG. 3. Phase diagram for a coadsorption system belonging to region a-a with $V_{11}/k_B=-1800$ K, $V_{22}/k_B=-1400$ K, $V_{12}/k_B=-2000$ K, $W_{11}/k_B=-1600$ K, $W_{22}/k_B=-800$ K, and $W_{12}/k_B=-250$ K.

IV. PHASE TRANSITIONS

As an example of the conditions under which phase transitions occur, we will discuss the one between $P6a$ and $P15a$, and $P15a$ and $F7$. The occupational configuration at the transition between $P6a$ and $P15a$ was numerically found to be at

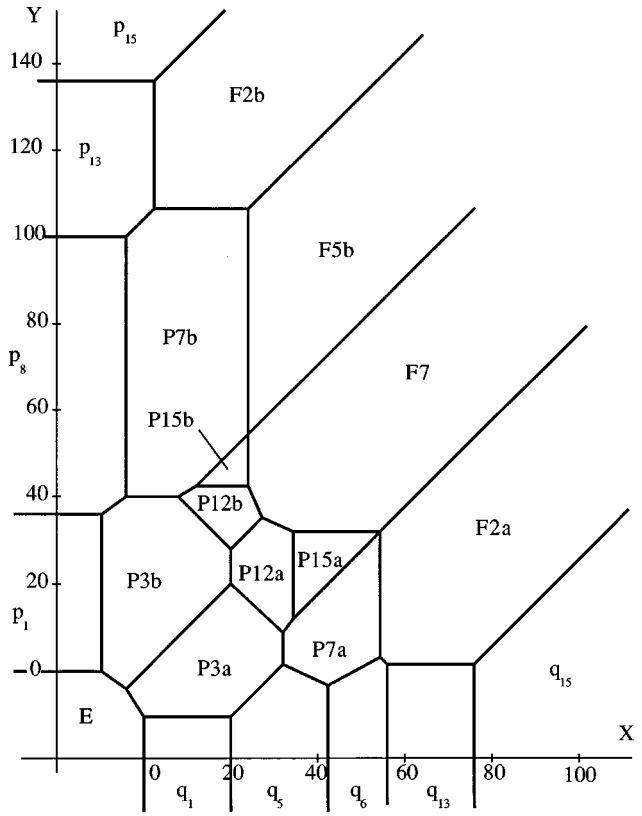

FIG. 4. Phase diagram for a coadsorption system belonging to region a-c with $V_{11}/k_B=-1800$ K, $V_{22}/k_B=-1400$ K, $V_{12}/k_B=-300$ K, $W_{11}/k_B=-1600$ K, $W_{22}/k_B=-500$ K, and $W_{12}/k_B=200$ K.

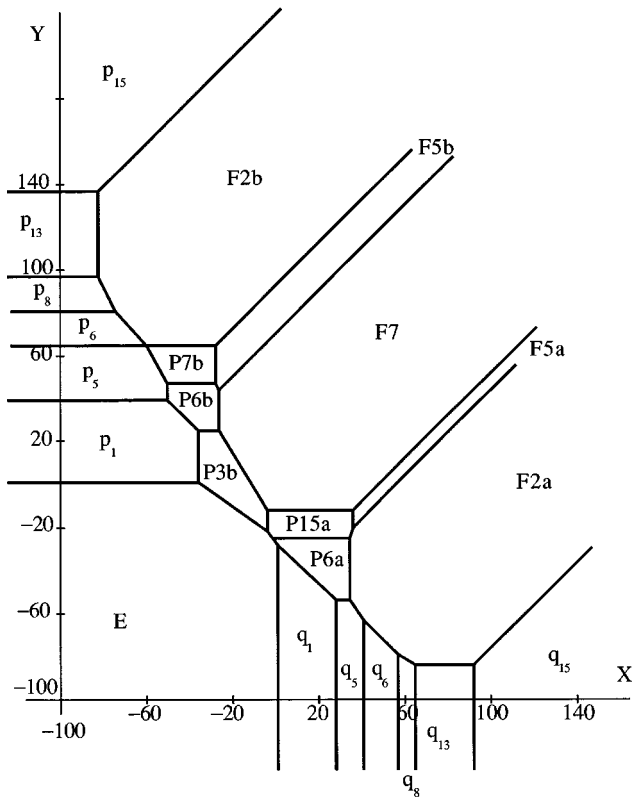

FIG. 5. Phase diagram for a coadsorption system belonging to region b-b with $V_{11}/k_B=-2400$ K, $V_{22}/k_B=-1600$ K, $V_{12}/k_B=1200$ K, $W_{11}/k_B=-1000$ K, $W_{22}/k_B=-700$ K, and $W_{12}/k_B=900$ K.

$$\theta_{10}=\tfrac{1}{4},\quad \theta_{20}=\tfrac{1}{2},\quad \theta_{11}=0,\quad \theta_{22}=\frac{M-1}{2M},$$
$$\theta_{12}=\tfrac{1}{2},\quad \beta_{11}=\beta_{22}=0,\quad \beta_{12}=\frac{M-1}{M}. \tag{11}$$

With this information, it is possible to compute the number C of possible lattice configurations satisfying these conditions. For simplicity, let us assume that the length N of the lattice is an integer multiple of 4, $N=4n$, with n being very large. All possible configurations are generated by having every other lattice strip of M sites (there are $2n$ of them) fully occupied by monomers of the second species, while the remaining $2n$ strips are equally divided into two possible configurations for which every other site of the M sites in a strip is occupied by a monomer of the first species: one has $(M+1)/2$ monomers and the other has $(M-1)/2$ monomers. There are only two possible ways of having every other strip fully occupied by monomers of the second species and there are $(2n)!/(n!)^2$ possible ways of having the remaining $2n$ strips equally distributed among the two configurations of $(M+1)/2$ and $(M-1)/2$ monomers of the second species. Thus $C=2(2n)!/(n!)^2$ and the value of the entropy S follows as

$$C=\frac{2(2n)!}{(n!)^2}=\frac{2^{2n+1}\Gamma(n+\frac{1}{2})}{\Gamma(\frac{1}{2})\Gamma(n+1)}, \tag{12}$$

$$S=\lim_{n\to\infty}\left(\frac{1}{4nM}\right)\ln\left(\frac{2^{2n+1}\Gamma(n+\frac{1}{2})}{\Gamma(\frac{1}{2})\Gamma(n+1)}\right)=\left(\frac{1}{2M}\right)\ln 2.$$

This expression has also been verified numerically.

The transition from $P15a$ to $F7$ was observed to occur at

$$\theta_{10}=\frac{3M+1}{8M},\quad \theta_{20}=\frac{1}{2},$$
$$\theta_{11}=\frac{M-1}{4M},\quad \theta_{22}=\frac{M-1}{2M},\quad \theta_{12}=\frac{3M+1}{4M}, \tag{13}$$
$$\beta_{11}=\beta_{22}=0,\quad \beta_{12}=\frac{M+1}{M}.$$

In this case, assume again that the length N of the lattice is a multiple of 4. Then every other of the $4n$ strips of M sites are still occupied by monomers of the second species, while the remaining $2n$ strips have monomers of the first species with the two edge sites in all strips being occupied. We focus on the configurations of the latter $2n$ strips, which we divide into n pairs, each pair satisfying the conditions of Eq. (13). One such pair is the one made of a strip (1) fully covered by M monomers of the first species, with the other (2) containing $(M+1)/2$ monomers of the same species having no first neighbors. This pair has a total of $(3M+1)/2$ monomers making a total of $M-1$ first neighbors; all the conditions of Eq. (13) are met. These are also met by removing k nonad-

jacent, nonedge monomers from strip 1 and placing them in the vacant sites of strip 2. Let $A_k(M)$ be the number of ways the k monomers can be removed. Each monomer removed decreases the number of nearest neighbors by 2, so that the number of first neighbors left is $M-2k$. After placing the k monomers in strip 2, other arrangements are possible that maintain $2k$ first neighbors. Let $B_k(M)$ be the number of such arrangements of $k+(M+1)/2$ monomers on a strip of M sites making $2k$ first neighbors, with the two edge sites occupied. The number of monomers removed from strip 1 to strip 2 should not exceed the integer part of $M/4$, or $[M/4]$, to avoid double counting. Straightforward combinatorial analysis shows that

$$A_k(M)=\sum_{J_k=1}^{M-2k}\sum_{J_{k-1}=1}^{J_k}\cdots\sum_{J_1=1}^{J_2}1,$$
$$B_k(M)=\sum_{J_{2k}=1}^{(M+1)/2-k}\sum_{J_{2k-1}=1}^{J_{2k}}\cdots\sum_{J_1=1}^{J_2}1,\quad k\leqslant\left[\frac{M}{4}\right], \tag{14}$$

with the initial conditions $A_0=B_0=1$. Thus a pair satisfying Eq. (13) could be chosen from any of the pairs generated above. It is possible to show that for the series of values of $M=4m+1$ (m being a positive integer), $A_{[M/4]}=B_{[M/4]}$, and the corresponding strip configurations are identical. In all cases including the latter one, the number of ways one may choose a pair of strips with $M-k$ monomers in one and $k+((M+1)/2)$ in the other, with the required first-neighbor condition and with the edge sites occupied, is A_kB_k. When there are i_k pairs made of these strips, the total number of ways of choosing them is $(A_kB_k)^{i_k}$. In general, consider the n pairs of strips occupied by monomers of the first species, with $i_0,i_1,\ldots,i_{[M/4]}$ pairs of strips having, M and $(M+1)/2$ monomers, $M-1$ and $(M+3)/2$ monomers,..., $M-[M/4]$ and $[M/4]+(M+1)/2$ monomers, respectively. One has

$$i_0+i_1+\cdots+i_{[M/4]}\equiv\{i\}=n. \tag{15}$$

The number of permutations of these $2n$ strips is $(2n)!$. To avoid the double counting of configurations, one has to divide that number by the following permutations: $i_0!$ for the i_0 strips that are fully occupied; another $i_0!$ for the i_0 strips that have every other site occupied including the edge sites; and $(2i_k)!$ for the $2i_k$ pairs, from $k=1$ to $[M/4]$, that is,

$$\frac{(2n)!}{(i_0!)^2(2i_1)!(2i_2)!\cdots(2i_{[M/4]})!}=\binom{2n}{i_0i_02i_12i_2\cdots2i_{[M/4]}}. \tag{16}$$

The total number C of configurations satisfying the conditions of Eq. (13) follows and

$$C=2\sum_{\{i\}=n}\left\{\binom{2n}{i_0i_02i_12i_2\cdots2i_{[M/4]}}\prod_{k=0}^{[M/4]}(A_kB_k)^{i_k}\right\}, \tag{17}$$
$$S=\lim_{n\to\infty}\frac{1}{4nM}\ln C.$$

Here $\{i\}=n$ means that the summation is carried over all the set of values of i_0 to $i_{[M/4]}$ satisfying Eq. (15). The overall factor of 2 in the expression of C follows from the fact that there are two distinct ways of having every other strip of the lattice fully occupied by monomers of the second species. The entropy at the transition between the phases $P15a$ and $F7$ using the matrix formulation of the problem for $M=5$ and 7 shows the value of S to have a closed-form expression,

TABLE IV. Infinite limit of the coadsorption phases listed in Tables I–III.

Phases (finite width)	2D	θ_{10}	θ_{20}	θ_{11}	θ_{22}	θ_{12}	β_{11}	β_{22}	β_{12}
p_1	$\overline{p_1}$	$\frac{1}{4}$	0	0	0	0	0	0	0
$p_5,p_8,P1b,P2b$	$\overline{p_2}$	$\frac{1}{2}$	0	0	0	0	1	0	0
p_6	$\overline{p_3}$	$\frac{1}{2}$	0	$\frac{1}{2}$	0	0	0	0	0
p_{13}	$\overline{p_4}$	$\frac{3}{4}$	0	1	0	0	1	0	0
$p_{15},F1b$	$\overline{p_5}$	1	0	2	0	0	2	0	0
q_1	$\overline{q_1}$	0	$\frac{1}{4}$	0	0	0	0	0	0
$q_5,q_8,P1a,P2a$	$\overline{q_2}$	0	$\frac{1}{2}$	0	0	0	0	1	0
q_6	$\overline{q_3}$	0	$\frac{1}{2}$	0	$\frac{1}{2}$	0	0	0	0
q_{13}	$\overline{q_4}$	0	$\frac{3}{4}$	0	1	0	0	1	0
$q_{15},F1a$	$\overline{q_5}$	0	1	0	2	0	0	2	0
$P3a,b;P4a,b;P11a,b;P12a,b$	$\overline{P1}$	$\frac{1}{4}$	$\frac{1}{4}$	0	0	0	0	0	1
$P10$	$\overline{P2}$	$\frac{1}{4}$	$\frac{1}{4}$	0	0	$\frac{1}{2}$	0	0	0
$P5a,P8a,P13a,P14a,P16b$	$\overline{P3}a$	$\frac{1}{4}$	$\frac{1}{2}$	0	0	1	0	1	0
$P6a,P7a,P15a$	$\overline{P4}a$	$\frac{1}{4}$	$\frac{1}{2}$	0	$\frac{1}{2}$	$\frac{1}{2}$	0	0	1
$P6b,P7b,P15b$	$\overline{P4}b$	$\frac{1}{2}$	$\frac{1}{4}$	$\frac{1}{2}$	0	$\frac{1}{2}$	0	0	1
$P5b,P8b,P13b,P14b,P16a$	$\overline{P3}b$	$\frac{1}{2}$	$\frac{1}{4}$	0	0	1	1	0	0
$P9a,F2a,F3a$	$\overline{F1}a$	$\frac{1}{4}$	$\frac{3}{4}$	0	1	1	0	1	1
$P17a,b;P18a,b;F4a,b;F6$	$\overline{F2}$	$\frac{1}{2}$	$\frac{1}{2}$	0	0	2	1	1	0
$F5a,b;F7$	$\overline{F3}$	$\frac{1}{2}$	$\frac{1}{2}$	$\frac{1}{2}$	$\frac{1}{2}$	1	0	0	2
$P9b,F2b,F3b$	$\overline{F1}b$	$\frac{3}{4}$	$\frac{1}{4}$	1	0	1	1	0	1

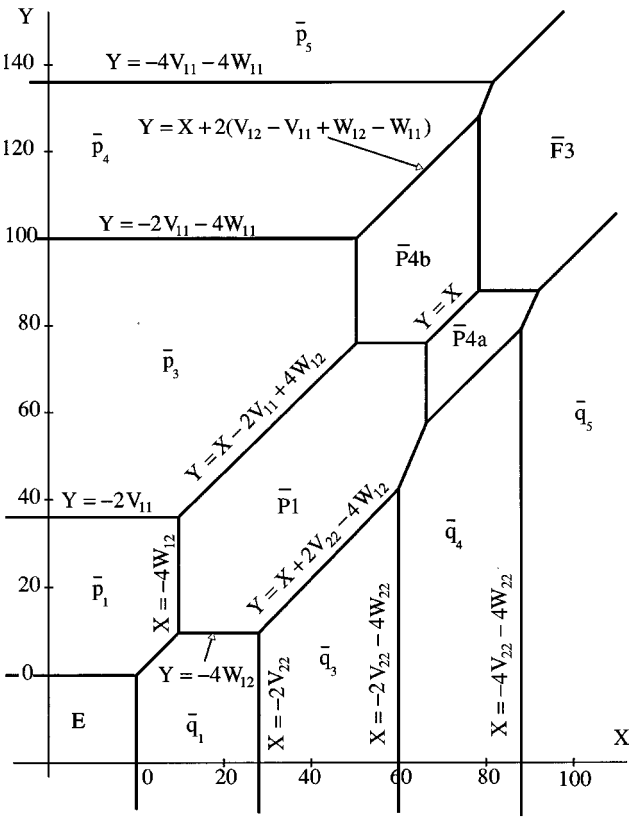

FIG. 6. Phase diagram for a coadsorption system on the infinite two-dimensional lattice with the same interaction energies as those of Fig. 3.

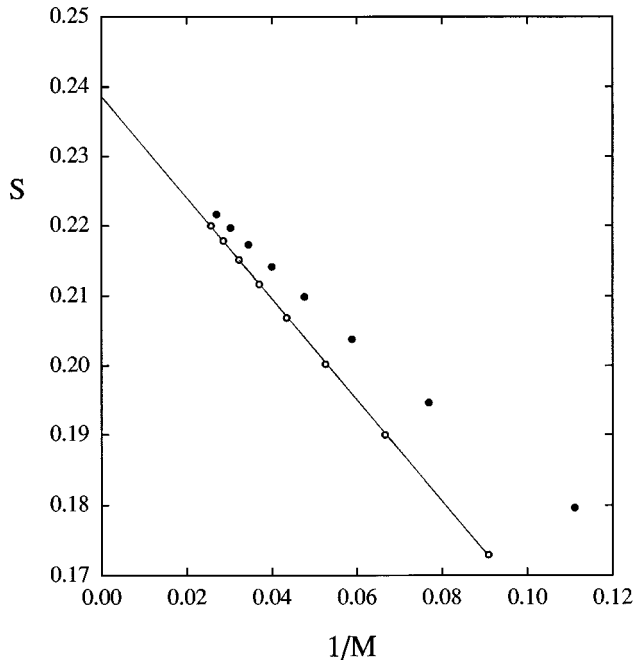

FIG. 7. Transition entropy per site divided by Boltzmann's constant S between phases $P15a$ and $F7$ plotted versus the reciprocal $1/M$ of the lattice width.

namely, $\frac{1}{10}\ln 5$ and $\frac{1}{14}\ln(2+\sqrt{30})$, respectively. These values were also verified numerically by applying Eq. (17). Using Eq. (17) up to $M=15$, numerical computations have shown S to approach the exact closed-form expression

$$S=\left(\frac{1}{2M}\right)\ln\left(2+\sum_{k=1}^{[M/4]}\sqrt{A_kB_k}\right). \tag{18}$$

A complete proof of this result for any M is lacking at this time.

V. THE INFINITE TWO-DIMENSIONAL LATTICE

In the previous sections, all the expressions obtained analytically in terms of odd M may be extended to $M=\infty$, thus providing the adsorption patterns, phase diagrams, and phase transitions on the infinite two-dimensional (2D) lattice. In this limit, one observes the merging of the phases as presented in Table IV. The single monomer species phase adsorption on the 2D lattice is that reported in Ref. [1]. Simple extrapolation of the phases involving a mixture of monomer species shows their merging into six partial coverage P phases and four full coverage F phases. Of these latter ten phases $P1$, $P2$, $F2$, and $F3$ are their own dual phases. They correspond to *equal* coverage of the lattice by each of the molecular species: $\frac{1}{4}$ in one case and $\frac{1}{2}$ in the other. The remaining mixture phases of unequal coverage include: four P phases with $\frac{1}{4}$ of the lattice covered by one of the species and $\frac{1}{2}$ by the other and two F phases with $\frac{1}{4}$ of the lattice covered by one species and $\frac{3}{4}$ by the other.

Figure 6 provides a sample of phase diagrams for a 2D lattice that is the infinite width limit of the phase diagram of Fig. 3. For convenience, equations of some of the boundary lines are shown, even though they are easily obtained using Eq. (9) and from the knowledge of the phases sharing the common boundary as listed in Table IV.

We will now discuss the conditions prevailing at a boundary between two phases and consider the infinite width limit of the two transitions discussed in Sec. IV. As one should expect, since phases $P6a$ and $P15a$ merge into phase $\bar{P}4a$ in the 2D limit as shown in Table IV, the characteristics of any point on the boundary line between these phases, given by Eqs. (11) and (12), merge with those of $P6a$ and $P15a$. A sample of a different behavior is the 2D limit of the phase transition between $P15a$ and $F7$, which become phases $\bar{P}4a$ and $\bar{F}3$. The conditions at the boundary between these latter phases are given by the infinite width limit of Eqs. (13) and (18). The occupational characteristics at the transition follow from Eq. (13) as

$$\theta_{10}=\tfrac{3}{8},\quad \theta_{20}=\tfrac{1}{2},\quad \theta_{11}=\tfrac{1}{4},\quad \theta_{22}=\tfrac{1}{2},\quad \theta_{12}=\tfrac{3}{4},$$

$$\beta_{11}=0,\quad \beta_{22}=0,\quad \beta_{12}=1. \tag{19}$$

However, we have been unable to obtain a closed-form expression in M of Eq. (18) providing the entropy S at the transition. Consequently, using Eq. (18), S was numerically computed for every odd value of M up to and including $M=39$. Figure 7 is a plot of S versus $1/M$. The data points follow two distinct series, corresponding to $M=4m+1$ and $M=4m+3$. The series of data points corresponding to $M=4m+3$ appears to be almost linear starting at $M=11$. Lin-

ear extrapolation to the infinite width of the set of eight data points (from $M=11-39$) provides the value of S on the 2D lattice to be 0.2384 with a correlation coefficient better than 0.9999.

VI. SUMMARY AND CONCLUSION

The low-temperature coadsorption phases of two monomer species on a semi-infinite square lattice of odd width M have been characterized. The assumption that first-neighbor interaction between monomers of the same species is repulsive while all other interaction energies may be attractive or repulsive is supported experimentally [4,5]. Based on the study of single-monomer adsorption [1], there are only 15 interaction energy regions to be studied. This results in numerous zero-entropy phases and possible phase diagrams. All the occupational configurations and some representative phase diagrams are presented and analyzed.

Using the continuity of energy per site across phase boundaries, one obtains the boundary-line equations in analytical form. At a transition, the entropy has a local maximum. From the numerically determined occupational configurations at a transition, we present a few cases where a closed-form expression for the transition entropy is obtained.

The occupational characteristics of all the phases are found to have closed-form analytic expressions in M, and straightforward extrapolation yields the phases and phase diagrams on the infinite two-dimensional lattice. The entropy at the transition between phases on the infinite lattice is also discussed.

Heterogeneous catalysis can be enhanced by coadsorption, partly justifying our study. For example, in the Fisher-Tröpsch process (carbon monoxide and hydrogen reduced catalytically to yield a mixture of alkanes), coadsorption of potassium with the carbon monoxide substantially increases the catalytic properties of the iron substrate [6]. Increased theoretical interest in coadsorption is exemplified by Ref. [7], in which phase $\overline{F}_2$ is studied for the coadsorption of carbon monoxide on nickel (100) with potassium (promoter) and with sulfur (poison). An additional example of the same phase $\overline{F}_2$ involves electrodeposition of silver onto platinum (100) with adsorbed iodine [8]. However, we have not been able to find experimental data showing a systematic search of all possible adsorption or coadsorption patterns of a given molecular species on a given surface. By holding one partial pressure constant and varying the other, data should provide the occupational configurations of the various phases encountered, and possibly the partial pressures at which transitions occur. Should this data become available, our model indicates that it will be possible to predict the values of adsorbate-adsorbate interaction energies. Perhaps first- and second-neighbor interactions would be sufficient to provide a complete explanation for the observed patterns. Third- and higher-order-neighbor interactions may still have a nonnegligible effect on adsorption patterns. Our model suggests that one could estimate these interactions using an extension of Eq. (9), provided the conditions of all phase transitions are determined experimentally.

One expects a phase diagram to be unique for a given adsorption or coadsorption system. Consequently, we have developed a MAPLE program allowing the geometrical construction of the family of phase diagrams assuming that the occupational characteristics of all possible phases are the only known parameters. Knowledge about other parameters, such as some of the conditions under which phase transitions occur, may be added as available to make definite predictions on first- and second-neighbor interactions.

Finally, this model may be particularly useful in the study of coadsorption on terraces [4], which also enhance catalytic activity [9]. For finite-width terraces, our model is exact provided interaction energies at the edges are negligible, and only first- and second-neighbor interactions are preeminent.

ACKNOWLEDGMENTS

We gratefully acknowledge support from the National Science Foundation and the Pittsburgh Supercomputing Center, Grant Nos. PHY910014P and SEE960012P.

[1] A. J. Phares and F. J. Wunderlich, Phys. Rev. E **55**, 2403 (1997).

[2] A. J. Phares, F. J. Wunderlich, D. W. Grumbine, Jr., and J. D. Curley, Phys. Lett. A **173**, 365 (1993); A. J. Phares, F. J. Wunderlich, J. D. Curley, and D. W. Grumbine, Jr., J. Phys. A **26**, 6847 (1993); A. J. Phares and F. J. Wunderlich, Phys. Lett. A **226**, 336 (1997).

[3] A. J. Phares, J. Math. Phys. (N.Y.) **25**, 1756 (1984).

[4] G. A. Somorjai, *Itroduction to Surface Chemistry and Catalysis* (Wiley, New York, 1994).

[5] S.-L. Chang and P. A. Thiel, Phys. Rev. Lett. **59**, 296 (1987).

[6] D. J. Dwyer and G. A. Somorjai, J. Catal. **52**, 291 (1978).

[7] E. Wimmer, C. L. Fu, and A. J. Freeman, Phys. Rev. Lett. **55**, 2618 (1985).

[8] J. L. Stickney, S. D. Rosasco, B. C. Schardt, and A. T. Hubbard, J. Chem. Phys. **88**, 251 (1984).

[9] K. Baron, D. W. Blakely, and G. A. Somorjai, Surf. Sci. **41**, 45 (1974).